Inclusion Compounds of Binaphthol with Lutidines − Structures, Selectivity and Kinetics of Desolvation

Elise de Vries,[a] Luigi R. Nassimbeni,[a] and Hong Su*[a]

Keywords: Inclusion compounds / Kinetics / Molecular recognition / Supramolecular chemistry / X-ray structure

The crystal structures of the inclusion compounds formed between the host 2,2′-dihydroxy-1,1′-binaphthyl (**BNP**) and three isomers of lutidine – 2,6-, 2,4-, and 3,5-lutidine – have been elucidated and their potential lattice energies calculated. The selectivities of enclathration by the host have been measured by competition experiments. The kinetics of desolvation of the inclusion compounds were studied and activation energies were determined. The results were reconciled in terms of the mode of inclusion and the lattice energies of the host–guest assemblies.

Introduction

Molecular recognition between a host compound and different guest compounds lies at the heart of host−guest chemistry, and has industrial applications such as the separation of close isomers, optical resolution and isolation of water-soluble materials, as reviewed by Toda.[1] Selective enclathration is the quintessential example of molecular recognition, as it depends on the matching of steric and electronic features in host and guest molecules to optimise the strengths and directions of noncovalent intermolecular interactions formed between them. The use of single-crystal X-ray diffraction yields refined crystal structure parameters and therefore facilitates the study of the assembly of host and guest molecules and the strengths of host-guest interactions. The ultimate goal of such structural analyses is to explain macrophenomena such as selectivity, thermal stability and kinetic behaviour of a particular compound in terms of intermolecular forces.

The host compound, 2,2′-dihydroxy-1,1′-binaphthyl (binaphthol, **BNP**), forms a large number of inclusion compounds with a variety of guest compounds,[2] since it is bulky and rigid, with a scissor-shaped backbone, and has functional hydroxy groups for effective guest binding. The X-ray structures of the unsolvated host compound **BNP** were elucidated for the racemic form as well as for both of the enantiomerically pure forms.[3,4] The optically active form of **BNP** is effective for the resolution of sulfoxides,[5] selenoxides[6] and amine *N*-oxides[7] etc. In addition, the resolved host **BNP** enclathrates a number of chiral guest compounds such as 1,2-cyclohexanediamine[8] and proline.[9] We have also used this host compound **BNP** to separate the isomers of picoline.[10] We now present studies of crystal structures, competition experiments, lattice energy calculations and kinetics of desolvation of this host with three isomers of lutidine.

[a] Department of Chemistry, University of Cape Town, Rondebosch 7701, South Africa
Fax: (internat.) + 27-21/685-4580
E-mail: xrayhong@psipsy.uct.ac.za

Results and Discussion

The inclusion compounds were obtained by dissolving the host compound **BNP** in the liquid 2,4-lutidine (**24L**), 2,6-lutidine (**26L**) and 3,5-lutidine (**35L**), respectively. Colourless crystals appeared on slow concentration over a period of 24 h. The results of thermal analyses using thermogravimetry (TG) and differential scanning calorimetry (DSC) are shown in Figure 1. For all of the three inclusion compounds, the TG analyses show a one-step desolvation, corresponding to the first endothermic peaks in the DSC. The last endothermic peak in the DSC corresponds to the melting of the apohost. The observed mass losses for each compound by TG are in good agreement with the calculated value, and thus endorse our acceptance of the host/guest ratios assigned for each of the inclusion compounds.

The host **BNP** formed 1:2 inclusion compounds with **26L** and **24L**. Both **BNP**·2(**26L**) (**1**) and **BNP**·2(**24L**) (**2**) crystallised in the *C*2/*c* space group, with four host and eight guest molecules per unit cell. The host molecules were therefore located on a diad at Wyckoff position *e*, and the guests were placed in general positions. These two structures are stabilised by host···guest hydrogen bonds with (host)O−H···N(guest) displaying O···N distances of 2.815(5) and 2.826(3) Å for **1** and **2**, respectively. The molecular structure of **1** is shown as an example in Figure 2 (a). Details of the hydrogen bonding for all the three structures are given in Table 1. In the crystal structure of **1**, the guests are located in channels parallel to [001], with an approximate cross-sectional area of 7 × 6 Å. In the crystal structure of **2**, the guest molecules are found in channels that run along [101] at $y = 0.25$ and 0.75, with an approximate cross-sectional area of 5 × 8 Å. A typical view of the channels of **2** is shown, as an example, in Figure 3. The packing diagrams of **1** and **2** are shown in Figure 4 (a and b, respectively).

The host formed a 1:1 inclusion compound with **35L**. Compound **BNP**·**35L** (**3**) crystallised in the $P(\bar{1})$ space group, with $Z = 2$. The host and guest molecules are in general positions. Each host molecule is hydrogen-bonded

  1434−193X/01/0510−1887 $ 17.50+.50/0

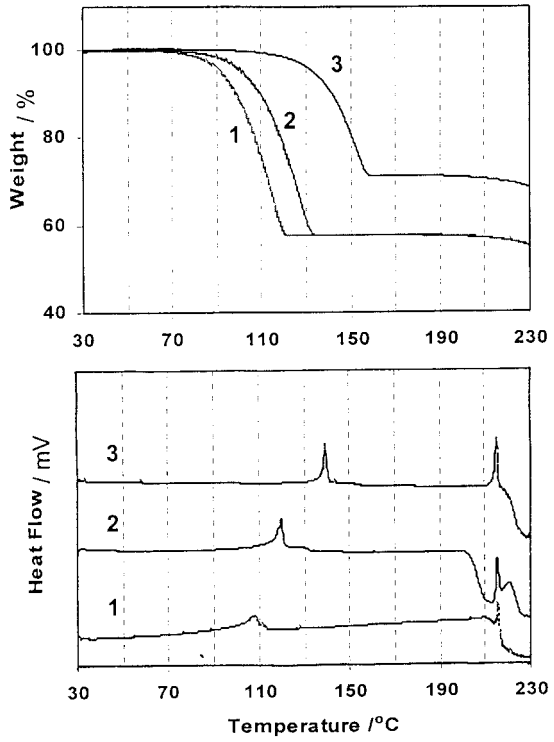

Figure 1. TG and DSC curves of **1** = **BNP**·2(**26L**), **2** = **BNP**·2(**24L**) and **3** = **BNP**·**35L**

to a guest molecule and another host molecule through a centre of inversion, displaying (host)O···N(guest) and (host)O···O(host) distances of 2.658(3) and 2.794(2) Å, respectively. The hydrogen-bonding scheme is represented graphically in Figure 2 (b). Details of the hydrogen bonding are given in Table 1. The guest molecules are again located in channels with a wave-like nature along [010], with an approximate diameter of 5 Å at the narrowest region and 7.5 Å at the widest. The crystal packing of **3** viewed down [010] is shown in Figure 4 (c).

The torsion angle C(2)−C(1)−C(11)−C(12) (as in **3**) and C(2)−C(1)−C(1)′−C(2)′ (as in **1** and **2**), which defines the conformation of the host, varies from 73.5(3)° in **2** through 77.4(7)° in **1** to 85.1(3)° in **3**. This is in general agreement with all the known crystal structures containing this host. A search of the Cambridge Structural Database System[11] produced 27 entries for this host molecule, with this torsion angle varying from 75° to 110°, and averaging 91°.

Competition experiments were performed to determine the enclathration selectivity of the host for these three lutidine isomers. The results are illustrated in Figure 5. Each two-component experiment shows the mol fraction X of a given guest in the initial solution versus the mol fraction Z of that guest included by the host. We note that **26L** and **24L** are both enclathrated in preference to **35L**. In the competition between **24L** and **26L**, concentration-dependent selectivity is observed and one of them is strongly favoured when its mol fraction (X) is greater than 0.5. Competition conducted with all three isomers simultaneously supported the results observed in the two-component competition experiments. The three-component experiment is shown in the

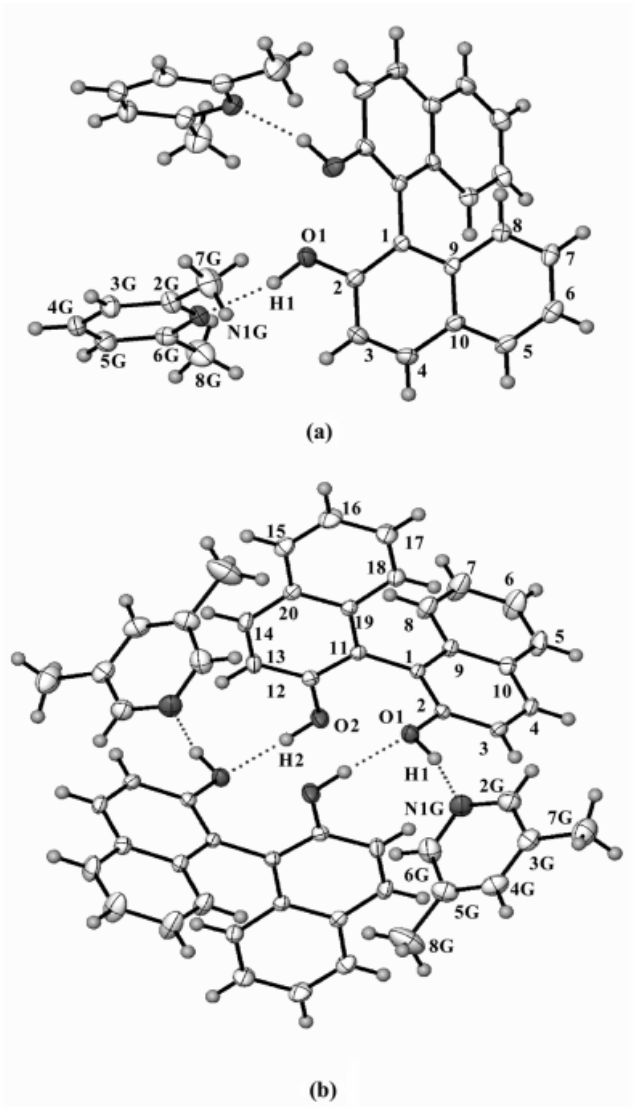

Figure 2. Molecular structures of **1** (a) and **3** (b) with atoms displayed as ellipsoids at probability of 30%, showing numbering scheme and hydrogen bonding as dotted lines

equilateral triangle, the three apices of which represent the pure lutidines. We selected starting mixtures represented by the dark areas and the resultant mixtures shown by the arrows. We note that for starting mixtures with $X_{\mathbf{26L}} > X_{\mathbf{24L}}$, there is a migration towards **26L**, with the remaining mixtures moving towards **24L**. Compound **35L** is disfavoured in all cases. Therefore, the host compound shows preferential enclathration selectivity with the lutidine isomers in the following order: **26L**·≈ **24L** > **35L**.

The potential energy environment of the guest molecules in the host structural environment was studied using empirical atom pair potentials. The program MPA[12] was employed to calculate intermolecular nonbonded interactions, using a force-field of the type

$$U(r) = a \cdot \exp(-br) - c/r^6$$

Table 1. Hydrogen bonding details

	Donor(**D**)−**H**···Acceptor(**A**)	**D**−**H**···**A** [Å]	**H**···**A** [Å]	**D**···**A** [Å]	**D**−**H**···**A** [°]
1	O1−H1···N1G	0.97(2)	1.87(2)	2.815(5)	164(4)
2	O1−H1···N1G	0.97(1)	1.876(8)	2.826(3)	165(2)
3	O1−H1···N1G	0.98(1)	1.69(1)	2.658(3)	166(3)
	O2−H2···O1[a]	0.96(1)	1.84(1)	2.794(2)	176(3)

[a] Symmetry codes: $-x + 2$, $-y + 1$, $-z + 1$.

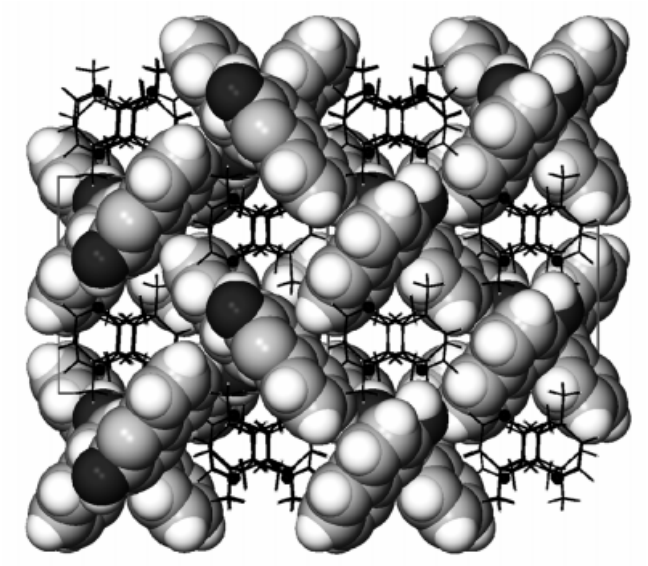

Figure 3. Space-filling projection of **2** along [101], showing the open channels; the guest molecules are represented as sticks, with nitrogen atoms as black circles; the host molecules are displayed with van der Waals radii

where r is the interatomic distance and the coefficients a, b and c are those given by Gavezzotti.[13] In each case the structure was allowed to relax and the minimised lattice energy was obtained. In addition, we incorporated a hydrogen-bonding potential which is a simplified form of that given by Vedani and Dunitz,[14] and is expressed as

$$U_{H\text{-}bond} = (A/R^{12} - C/R^{10}) \cos^2\theta$$

where R is the distance between the hydroxy hydrogen atom and the N acceptor, θ is the O−H···N angle and the $\cos^2\theta$ term is the energy penalty paid by the bond for nonlinearity. We carried out summations of the non-hydrogen-bonding lattice energies and the hydrogen-bonding potentials, and obtained the following values: −494.2 kJ mol^{-1} (**1**), −495.1 kJ mol^{-1} (**2**), −353.2 kJ mol^{-1} (**3**). It is interesting to note that the hydrogen-bonding interaction is, in fact, stronger for **3**, in which the (host)O···N(guest) distance of 2.658 Å is considerably shorter than that present in the other two compounds (2.815 and 2.826 Å). However, this is not the only factor contributing to the lattice energy, which also incorporates all other nonbonded interactions. We also note that the host/guest ratio is different in the compounds **1** and **2**, compared to **3**. This is also an important factor impinging on the values of the lattice energy. The

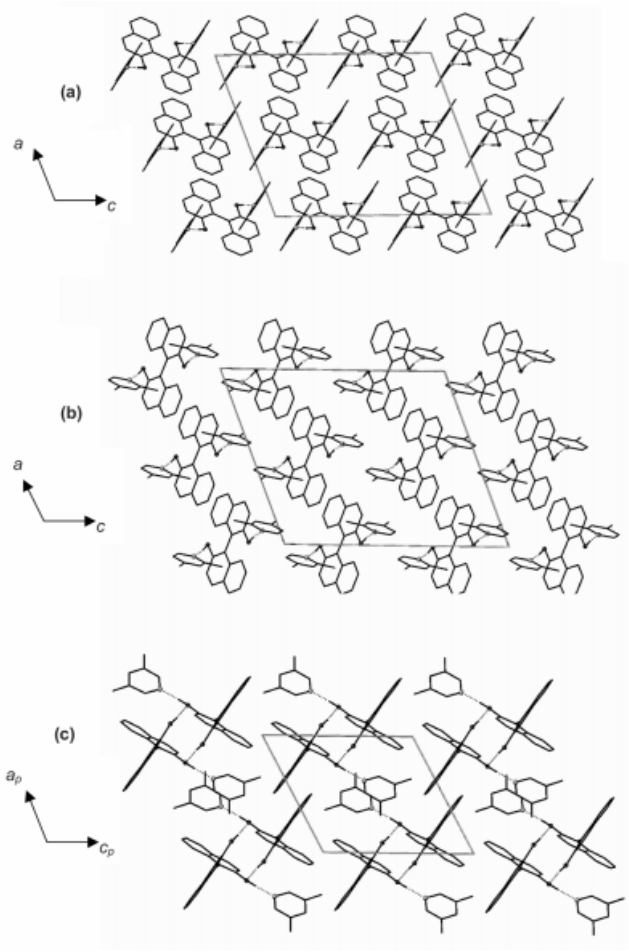

Figure 4. Projection along [010] for **1** (a), **2** (b) and **3** (c); the hydrogen bonding is shown as dotted lines; the oxygen atoms of the host are shown as solid circles and the nitrogen atoms of the guest as grey circles; all hydrogen atoms are omitted, except for the hydroxy hydrogen atoms of the host

results of lattice energy show that the stabilities of the three inclusion compounds are in the order **2**·≈ **1** > **3**. This explains the least preferred enclathration selectivity of **35L** by the host compound and the concentration-dependent selectivity between **1** and **2**. We note that in the case of separation of 3- and 4-picoline by the host 1,1′-bis(4-hydroxyphenyl)-cyclohexane,[15] where the lattice energy values were nearly equal, there was no selectivity of either isomer. We may attribute this phenomenon to kinetic effects.

We have analysed the kinetics of desolvation of all of the three inclusion compounds by carrying out a series of isothermal TG runs at selected temperatures. For the desolva-

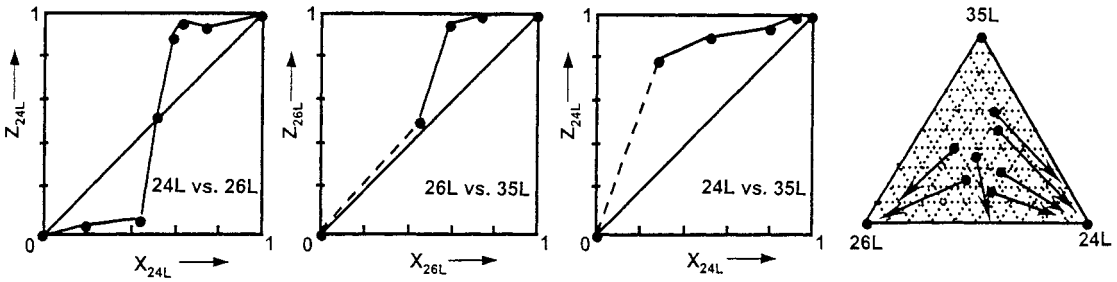

Figure 5. Results of the competition experiments

tion of **1** and **2**, the resultant curves of the extent of reaction α versus time t were deceleratory and were best fitted to the kinetic model R2.[16] The contracting area geometrical model R2 describes a phase boundary controlled reaction that reacts from the edge inward on a cylindrical particle. The rate equation of R2 is stated as:

$$1 - (1 - \alpha)^{1/2} = kt$$

For the desolvation of **3**, sigmoid α-time curves were obtained and were best fitted to the Avrami−Erofe'ev model A3, which has the form $[-\ln (1 - \alpha)]^{1/3} = kt$. The Arrhenius plots, ln k versus $1/T$, are plotted for the desolvation reactions of each of the inclusion compounds as shown in Figure 6. This yielded an activation energy E_a and a pre-exponential factor ln A for each compound as follows: E_a = 80(4) kJ mol^{-1}, ln A = 24(1) (**1**); E_a = 92(3) kJ mol^{-1}, ln A = 7(2) (**2**); E_a = 101(7) kJ mol^{-1}, ln A = 28(2) (**3**).

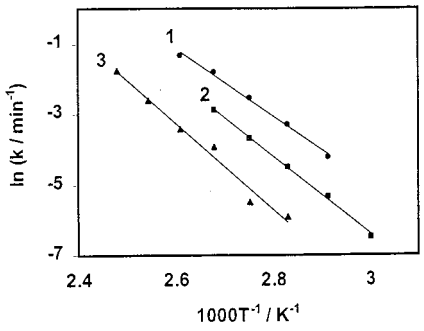

Figure 6. Arrhenius plots of ln k vs. $1/T$ for the desolvation reactions of all three inclusion compounds

A comparison of the kinetics of desolvation for a particular host compound with different guest compounds[17] suggested that E_a is related to the mode of inclusion of the guest. An E_a of the range 60−150 kJ mol^{-1} has been observed for the channel-type inclusion compounds,[18,19] which are generally lower than guest inclusion within cavities. This result would be expected since the guest molecules in channels have small physical barriers allowing facile diffusion out of the host lattice. The E_a values obtained here fall in the small range 80−110 kJ mol^{-1}, similar to those observed for other channel-type inclusion compounds with the same host **BNP**.[12,20]

Conclusion

The crystal structures of **1**, **2** and **3** were elucidated. Studies of the inclusion mode of the guest molecules within the host framework were correlated with the activation energies of the desolvation reactions of these three inclusion compounds. The potential lattice energies were calculated, and the relative stabilities indicated by these values agreed well with the observed selectivity trends of the host compound.

Experimental Section

General Remarks: TG and DSC were carried out with a Perkin−Elmer PC7 series system. These experiments were performed over a temperature range of 30−230 °C at a heating rate of 10 °C min^{-1} with a purge of dry nitrogen flowing at 30 mL min^{-1}. The samples were crushed, blotted dry and placed in open platinum pans for TG experiments and in crimped but vented aluminium pans for DSC. Data for the isothermal kinetics of desolvation were obtained from TG at selected temperatures. − Competition experiments were carried out between pairs of guests as follows: A series of 9 vials was made up, with mixtures of two guests such that the mol fraction of a given guest varied from 0 to 1. The host was added in the mixture and allowed to dissolve by warming. The total guest/host ratio was kept at 20:1 in each case. The mixtures were allowed to cool and to concentrate slowly. The resulting crystalline inclusion compounds were filtered, dried and dissolved in chloroform; these, together with the mother liquors from which the crystals had been obtained, were analysed by gas chromatography. This experiment was extended to investigate simultaneous competition by all three isomers. Initial compositions of all three guest mixtures were judiciously selected in order to sample the three guest components. The obtained crystalline inclusion compounds, as well as the mother liquors, were analysed as before.

X-ray Crystallographic Study: For all three inclusion compounds, single crystals of suitable size and distinct optical qualities were selected and mounted in Lindemann capillary tubes sealed together with a drop of mother liquor to minimise deterioration of the crystals caused by guest desorption. Preliminary cell dimensions and space group symmetry were determined photographically and subsequently refined with a Nonius Kappa CCD diffractometer, using graphite-monochromated Mo-K_α radiation. The strategy for data collection was evaluated using COLLECT software, scaled and re-

Table 2. Details for crystal data, data collection and refinement

Inclusion compound	**1**	**2**	**3**
Empirical formula	$C_{20}H_{14}O_2{\cdot}2C_7H_9N$	$C_{20}H_{14}O_2{\cdot}2C_7H_9N$	$C_{20}H_{14}O_2{\cdot}C_7H_9N$
Molecular mass [g mol^{-1}]	500.62	500.62	393.46
Crystal system	monoclinic	monoclinic	triclinic
Space group	*C*2/*c*	*C*2/*c*	$P\bar{1}$
a [Å]	14.656(7)	15.12(2)	10.341(1)
b [Å]	10.703(2)	10.76(1)	10.511(1)
c [Å]	18.365(5)	18.19(5)	11.868(1)
α [°]	90	90	103.651(5)
β [°]	109.84(3)	110.9(1)	113.502(2)
γ [°]	90	90	102.496(5)
V [Å^3]	2710(2)	2764(9)	1077.6(2)
Z	4	4	2
$D_{calcd.}$ [g cm^{-3}]	1.227	1.203	1.213
F(000)	1064	1064	416
λ [Å]	0.71073	0.71073	0.71073
T [K]	293	173	293
μ [mm^{-1}]	0.076	0.075	0.076
Scan range θ [°]	2.36−24.95	2.88−27.27	2.01−26.31
Data collection method	θ/2θ scans	θ/2θ scans	θ/2θ scans
Absorption correction (T_{min}/T_{max})	none	0.9780/0.9889	0.9702/0.9776
No. of measured reflections	11871	13552	4660
No. of independent reflections	2376	2665	3479
No. of observed reflections	937	1719	2186
Criterion for observed reflections	$I > 2\sigma(I)$	$I > 2\sigma(I)$	$I > 2\sigma(I)$
R_{int}	0.072	0.031	0.021
Index range, *h*/*k*/*l*	0,17/±12/−21,20	−11,17/−9,13/−21,16	±12/±9/−14,10
Final *R* indices [$F_o > 4(F_o)$], *R*1	0.054	0.0472	0.0515
*wR*2 (F^2)	0.1097	0.1072	0.1039
R indices (all data)	0.2208	0.0892	0.0972
Goodness of fit on F^2, *S*	1.083	1.037	1.024
No. of reflections used in refinement	2376	2665	3479
No. of parameters used	177	177	282
Weighting scheme	$w = 1/[\sigma^2(F_o^2) +$	$w = 1/[\sigma^2(F_o^2) +$	$w = 1/[\sigma^2(F_o^2) +$
$[P = (F_o^2 + 2F_c^2)/3]$	$(0.0359P)^2 + 4.22P]$	$(0.0568P)^2 + 0.47P]$	$(0.0401P)^2 + 0.35P]$
$(\Delta/\sigma)_{max}$	0.001	0.000	0.009
Max/min height Δρ in difference electron map [e Å^{-3}]	0.25/−0.22	0.20/−0.16	0.17/−0.15
Extinction coefficient	0.003(5)	0.0035(6)	0.018(2)
Source of atomic scattering factors	*International Tables for Crystallography*, **1992**, vol. C, Tables 4.2.6.8 and 6.1.1.4		

duced with DENZO-SMN software.[21] Salient crystal and experimental data are given in Table 2. Crystal structures were solved by direct methods using SHELX-86[22] and refined employing full-matrix least squares with the program SHELX-97,[23] refining on F^2. Molecular structure drawings and packing diagrams were produced using the program X-seed.[24] All non-hydroxy H atoms were placed geometrically and refined with riding model with the U_{iso} constrained to be 1.2 times that of U_{eq} of their parent atoms. The hydroxy H atoms of the host were located in difference electron-density maps and refined with simple bond-length constraints and independent isotropic temperature factors. The methyl groups of the guest of **2** were disordered and refined with two positions of the hydrogen atoms. Crystallographic data (excluding structure factors) for the structures reported in this paper have been deposited with the Cambridge Crystallographic Data Centre as supplementary publication nos. CCDC-157114 to -157116. Copies of the data can be obtained free of charge on application to CCDC, 12 Union Road, Cambridge CB2 1EZ, UK [Fax: (internat.) + 44-1223/336-033; E-mail: deposit@ccdc.cam.ac.uk].

[1] F. Toda, *Comprehensive Supramolecular Chemistry* (Eds.: D. D. MacNicol, F. Toda, R. Bishop), Pergamon, Oxford, **1996**, vol. 6, chapter 15.

[2] E. Weber, *Inclusion Compounds* (Eds.: J. L. Atwood, J. E. D. Davies, D. D. MacNicol), Oxford University Press, Oxford, **1991**, vol. 4, p. 213−223.

[3] F. Toda, K. Tanaka, H. Miyamoto, H. Koshima, I. Miyahara, K. Hirotsu, *J. Chem. Soc., Perkin Trans. 2* **1997**, 1877−1885.

[4] K. Mori, Y. Masuda, S. Kashino, *Acta Crystallogr., Sect. C* **1993**, *49*, 1224−1227.

[5] F. Toda, K. Tanaka, S. Nagamatsu, *Tetrahedron Lett.* **1984**, *25*, 4929−4932.

[6] F. Toda, K. Mori, *J. Chem. Soc., Chem. Commun.* **1986**, 1357−1359.

[7] F. Toda, K. Mori, Z. Stein, I. Goldberg, *Tetrahedron Lett.* **1989**, *30*, 1841−1844.

[8] S. Fukushima, H. Hosomi, S. Ohba, M. Kawashima, *Acta Crystallogr., Sect. C* **1999**, *55*, 120−123.

[9] M. Pariasamy, L. Venkatraman, K. R. J. Thomas, *J. Org. Chem.* **1997**, *62*, 4302−4306.

[10] L. R. Nassimbeni, H. Su, *Acta Crystallogr., Sect. B*, in press.

[11] CSDS, *Cambridge Structural Database System, Version 5.18*, Cambridge Crystallographic Data Centre, Cambridge, UK, **1999**.

[12] D. E. Williams, *MPA: Molecular Packing Analysis, Version 2*, Department of Chemistry, University of Louisville, Louisville, KY 40292, **1999**.

[13] A. Gavezzotti, *Crystallogr. Rev.* **1998**, *7*, 5−21.

[14] A. Vedani and J. D. Dunitz, *J. Am. Chem. Soc.* **1985**, *107*, 7653−7658.

[15] M. R. Caira, A. Horne, L. R. Nassimbeni, F. Toda, *J. Mater. Chem.* **1997**, *7*, 2145−2149.

[16] M. E. Brown, *Introduction to Thermal Analysis − Techniques and Applications*, Chapman and Hall, London, **1988**.
[17] L. R. Nassimbeni, *Molecular Recognition and Inclusion* (Ed.: A. W. Coleman), Kluwer Academic Publishers, Dordrecht, **1998**, p. 135−152.
[18] J. L. Scott, *J. Chem. Crystallogr.* **1996**, *26*, 185−189.
[19] M. R. Caira, A. Coetzee, L. R. Nassimbeni, E. Weber, A. Wierig, *J. Chem. Soc., Perkin Trans. 2* **1997**, 237−240.
[20] L. R. Nassimbeni, H. Su, *J. Phys. Org. Chem.* **2000**, *13*, 361−367.
[21] Z. Otwinowski, W. Minor, *Methods in Enzymology, Macromolecular Crystallography* (Eds.: C. W. Carter, Jr., R. M. Sweet), part A, vol. 276, Academic Press, **1997**, p. 307−326.
[22] G. M. Sheldrick, *SHELX-86*: *Crystallographic Computing* (Ed.: G. M. Sheldrick, C. Kruger, R. Goddard), Oxford University Press: Oxford, UK, **1985**, vol 3, p. 175.
[23] G. M. Sheldrick, *SHELX-97, Programme for Crystal Structure Determination*, University of Göttingen, Germany, **1997**.
[24] L. J. Barbour, *X-Seed: a graphical interface for the SHELX programme*, University of Missouri, Columbia, USA, **1999**.
Received November 29, 2000
[O00605]